JOURNAL OF AIRCRAFT
Vol. 48, No. 6, November–December 2011

# Reliability-Based Design of Representative Wing and Tail System Together with Structural Tests

Erdem Acar*
*TOBB University of Economics and Technology, 06560 Ankara, Turkey*

DOI: 10.2514/1.C031481

**Most reliability-based optimization studies focus on variables that are available in the design stage. However, it has been shown that inclusion of postdesign measures, such as structural tests and health monitoring, can lead to better design choices. More recently, a new reliability-based design framework that can include both predesign and postdesign uncertainty-reduction variables has been proposed in an earlier work. The present study elaborates on that study by including the system reliability considerations. A representative wing and tail system is considered in this study, and the wing and the tail are designed together with their corresponding structural tests. The number of coupon tests, the number of structural element tests, and the additional company knockdown factors for each component are selected as design variables to perform system reliability-based optimization for minimum direct operating cost. It is found that the optimum company knockdown factor for the wing is larger than that of the tail, because a small fraction of the wing material is moved to tail for optimal reliability allocation. It is also found that the optimum number of structural element tests for the wing is larger than or equal to that of the tail. Finally, the optimum number of coupon tests for the wing is found to be smaller than that of the tail.**

## Nomenclature

| | | |
|---|---|---|
| $A$ | = | load-carrying area of the most critical part of the wing or tail structure |
| $A_{\text{nom}}$ | = | nominal value of $A$ |
| $C_c$ | = | cost of coupon tests |
| $C_e$ | = | cost of element tests |
| $C_{\text{test}}$ | = | overall cost of tests |
| DOC | = | direct operating cost (life-cycle cost) |
| $k_f$ | = | additional company knockdown factor at the structural level (nominal value is taken as 0.95) |
| $N_a$ | = | number of aircraft in a fleet (taken as 1000) |
| $N_{\text{elem}}$ | = | number of different types of structural elements tested (taken as 100) |
| $N_{\text{mat}}$ | = | number of materials for which coupon testing is done (taken as 80) |
| $n_c$ | = | number of coupon tests (nominal value is taken as 50) |
| $n_e$ | = | number of element tests (nominal value is taken as 3) |
| $p$ | = | cost savings by reducing the structural weight by one unit |
| $P_f$ | = | probability of failure of a component |
| $(P_f)_{\text{W\&T}}$ | = | probability of simultaneous failure of the wing and the tail |
| $P_{\text{FS}}$ | = | probability of failure of the representative system composed of a wing and a tail |

*Subscripts*

| | | |
|---|---|---|
| $T$ | = | tail |
| $W$ | = | wing |

Presented at the 52nd AIAA/ASME/ASCE/AHS/ASC Structures, Structural Dynamics, and Materials Conference, Denver, CO, 4–7 April 2011; received 21 April 2011; revision received 26 May 2011; accepted for publication 27 June 2011. 

*Assistant Professor, Mechanical Engineering; acar@etu.edu.tr. Senior Member AIAA.

## I. Introduction

THE safety of aircraft structures can be achieved by designing the structure against uncertainty and by taking steps to reduce the uncertainty. In traditional reliability-based optimization, all uncertainties that are available at the design stage are considered in calculating the reliability of the structure (e.g., [1–14]). However, the effects of postdesign measures (e.g., structural tests, health monitoring activities) that can effectively reduce uncertainties are usually not included. It has been argued that it would be beneficial to include the effects of these uncertainty-reduction measures in the design process [15–18]. In this paper, the main focus is placed on the structural tests as a representative example of uncertainty-reduction measures.

There are few papers in the literature that address the effect of tests on structural safety. Jiao and Moan [19] investigated the effect of proof tests on structural safety using Bayesian updating. They showed that the proof testing reduces the uncertainty in the strength of a structure, thereby leading to substantial reduction in probability of failure. Jiao and Eide [20] explored the effects of testing, inspection and repair on the reliability of offshore structures. Beck and Katafygiotis [21] addressed the problem of updating a probabilistic structural model using dynamic test data from the structure by using Bayesian updating. Similarly, Papadimitriou et al. [22] used Bayesian updating within a probabilistic structural analysis tool to compute the updated reliability of a structure using test data. They found that the reliabilities computed before and after updating were significantly different.

In an earlier paper [23], the aforementioned studies on the effect of tests on structural safety [19–22] were extended in simulating all possible outcomes of future tests, which would allow the designer to design the tests together with the structure. In [24] a new reliability-based optimization framework was proposed that can include both predesign and postdesign uncertainty-reduction variables to design an aircraft structure together with its structural tests. The number of coupon tests was used as the predesign variable, the number of structural element tests as postdesign variable. In addition, it was assumed that in addition to satisfying a constraint on the probability of failure, the designer needs to satisfy the FAA (Federal Aviation Administration) regulations for deterministic design. To reconcile the two requirements, the fact that companies often apply additional knockdown factors to design allowables beyond the FAA requirements was used. The company knockdown factor was used as another design variable that modulates the tradeoff between cost and safety. It has been shown in [24] that the number of coupon and

element tests as well as the company knockdown factor can be selected in an optimal way to minimize the direct operating cost without jeopardizing the structural safety. However, in that study a sizing optimization problem is considered, and it is assumed that structural design of the aircraft is driven by the design of the most critical component, while the system reliability considerations has been left out, and this paper aims to fill this gap.

In this paper, sizing optimization of a representative wing and tail system is considered. The reliability-based optimization framework developed in [24] is extended to take system reliability considerations into account. It is assumed that the optimization of the wing and the tail are driven by their most critical components. The wing and the tail are designed together with their corresponding structural tests. The number of coupon tests, the number of element tests and the additional knockdown factor for each component are selected as design variables to perform system reliability-based optimization for minimum direct operating cost. The paper is organized as follows. Section II presents the formulation of the optimization problem for minimum direct operating cost. Section III presents a list of assumptions, simplifications and limitations of this work. Section IV discusses the safety measures taken during aircraft structural design. Section V first presents a simple uncertainty classification that divides uncertainties into two categories: errors and variability. Section V then discusses modeling of errors and variability throughout the design and testing of an aircraft, and probability of failure calculation. Finally, the system reliability-based optimization results and the concluding remarks are given in the last two sections of the paper, respectively.

## II. Optimization for Minimum Direct Operating Cost

As noted earlier, the main objective of the paper is to perform reliability-based design of a representative wing and tail system together with structural tests. The design variables of the optimization problem are chosen as the additional company knockdown factor $k_f$, the number of coupon tests $n_c$, and the number of element tests $n_e$. Since these variables may change from the wing to the tail, there exist six design variables $(k_f)_W$, $(n_c)_W$, $(n_e)_W$, $(k_f)_T$, $(n_c)_T$, and $(n_e)_T$, where the subscripts $W$ and $T$ correspond to the wing and the tail, respectively. The reliability-based design of a representative wing and tail system for minimum direct operating cost (DOC) can be performed by solving the following optimization problem:

Find

$$(k_f)_W, (n_c)_W, (n_e)_W, (k_f)_T, (n_c)_T, (n_e)_T \tag{1a}$$

Minimize

$$\mathrm{DOC}\,[(k_f)_W, (n_c)_W, (n_e)_W, (k_f)_T, (n_c)_T, (n_e)_T] \tag{1b}$$

Subject to

$$P_{\mathrm{FS}}[(k_f)_W, (n_c)_W, (n_e)_W, (k_f)_T, (n_c)_T, (n_e)_T] \le (P_{\mathrm{FS}})_{\mathrm{nom}} \tag{1c}$$

$$\begin{aligned} 0.8 \le (k_f)_W \le 1.0, \qquad & 0.8 \le (k_f)_T \le 1.0 \\ 30 \le (n_c)_W \le 100, \qquad & 30 \le (n_c)_T \le 100 \\ 1 \le (n_e)_W \le 5, \qquad & 1 \le (n_e)_T \le 5 \end{aligned} \tag{1d}$$

The $(P_{\mathrm{FS}})_{\mathrm{nom}}$ term in the constraint is the value of $P_{\mathrm{FS}}$ when the design variables take their nominal values (i.e., $(k_f)_W = (k_f)_T = 0.95$, $(n_c)_W = (n_c)_T = 50$, and $(n_e)_W = (n_e)_T = 3$). These nominal values are taken from an earlier work [24].

The cost model used in this study is also taken from [24]. The cost model is based on the paper by Kaufmann et al. [25]. The direct operating cost of the aircraft structure is defined as

$$\mathrm{DOC} = pW + C_{\mathrm{test}} \tag{2}$$

Here, $p$ is the total cost savings attained by reducing the structural weight $W$ by one unit, and $C_{\mathrm{test}}$ is the cost of tests. Since this study focuses mainly on the coupon tests and the element tests, the term $C_{\mathrm{test}}$ can be rewritten as

$$C_{\mathrm{test}} = C_c + C_e \tag{3}$$

where $C_c$ is the cost of coupon tests, $C_e$ is the cost of element tests. Equations (2) and (3) can be combined to yield

$$\mathrm{DOC} = pW + C_c + C_e \tag{4}$$

The total direct operation cost of the wing and tail system can be written as

$$\begin{aligned} &\mathrm{DOC}[(k_f)_W, (n_c)_W, (n_e)_W, (k_f)_T, (n_c)_T, (n_e)_T] \\ &\quad = \mathrm{DOC}_W[(k_f)_W, (n_c)_W, (n_e)_W] \\ &\qquad + \mathrm{DOC}_T[(k_f)_T, (n_c)_T, (n_e)_T] \end{aligned} \tag{5}$$

where $\mathrm{DOC}_W$ and $\mathrm{DOC}_T$ are the direct operation cost of the wing and the tail, and they can be formulated as

$$\begin{aligned} \mathrm{DOC}_W[(k_f)_W, (n_c)_W, (n_e)_W] &= pW_W((k_f)_W, (n_c)_W, (n_e)_W) \\ &\quad + C_c[(n_c)_W] + C_e[(n_e)_W] \end{aligned} \tag{6}$$

$$\begin{aligned} \mathrm{DOC}_T[(k_f)_T, (n_c)_T, (n_e)_T] &= pW_T((k_f)_T, (n_c)_T, (n_e)_T) \\ &\quad + C_c[(n_c)_T] + C_e[(n_e)_T] \end{aligned} \tag{7}$$

where $W_W$ and $W_T$ are the structural weights of the wing and the tail. Details of each term in the cost equation are provided below.

### A. Weight Penalty *p*

Curran et al. [26] proposed that the economical value of weight savings is 300/kg. Similarly, Kim et al. [27] referred to a recent report by the U.S. National Materials Advisory Board [28] that estimated that a 1 lb weight reduction amounts to a total savings of $200 for a civil transport aircraft. Jenkinson et al. [29] noted that operating cost of carrying an additional 1 lb over the lifetime of a 300–600-seat civil aircraft is around $1000. In this study, the weight penalty is varied between 100/lb and 1000/lb, and its effect on the optimization results is explored.

### B. Structural Weights of the Wing and the Tail

Jenkinson et al. [29] provided component weight estimations for typical civil aircraft normalized with the maximum takeoff weight (MTOW), and noted that the structural weight of a typical wing was about 10 to 12% of the MTOW, and the structural weight of a tail is about 1.5 to 3% of the MTOW. In this paper, the ratio of the wing weight to the MTOW and the ratio of tail weight to the MTOW are taken as $W_W/\mathrm{MTOW} = 10\%$ and $W_T/\mathrm{MTOW} = 2\%$, respectively.

In this paper, a typical civil transport aircraft with an MTOW of 300,000 lb is considered. The weights of the wing and the tail are then taken as 30,000 lb and 6000 lb, respectively. Since the test costs can be attributed to fleet of aircraft rather than a single one, total structural weight of the fleet is considered. Therefore, the weight terms $W_W$ and $W_T$ in Eqs. (6) and (7) can be written as

$$\begin{aligned} W_W[(k_f)_W, (n_c)_W, (n_e)_W] &= \frac{A[(k_f)_W, (n_c)_W, (n_e)_W]}{A_{\mathrm{nom}}} \\ &\quad \times N_a \times 30,000 \text{ lb} \end{aligned} \tag{8}$$

$$W_T[(k_f)_T, (n_c)_T, (n_e)_T] = \frac{A[(k_f)_T, (n_c)_T, (n_e)_T]}{A_{\mathrm{nom}}} \times N_a \times 6000 \text{ lb} \tag{9}$$

Here, $A$ is the load-carrying area, and $A_{\mathrm{nom}}$ is the value of $A$ when the design variables take their nominal values. It is assumed that a typical airliner has a production line of 1000 aircraft before it is discontinued or substantially redesigned, so $N_a = 1000$.

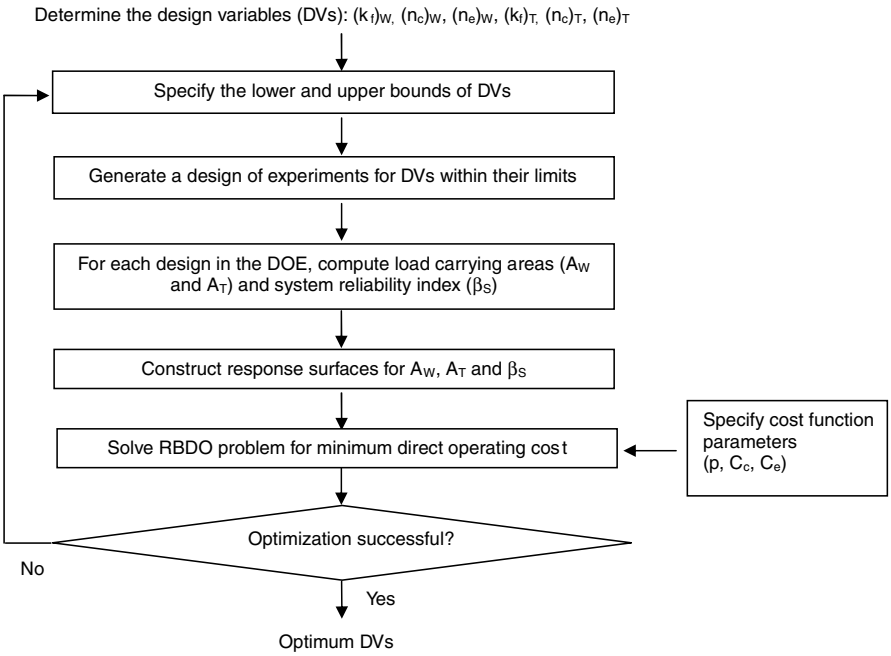


**Fig. 1 Flowchart for RBDO.**

### C. Test Costs

The costs[†] for the coupon tests and element tests are taken as \$300 for each coupon in a coupon test, and \$150,000 for each element tests. Accordingly, the respective costs are given (in dollars) as

$$C_c(n_c) = 300 \times N_{\text{mat}} \times n_c \tag{10}$$

$$C_e(n_e) = 150,000 \times N_{\text{elem}} \times n_e \tag{11}$$

where $N_{\text{mat}}$ is the number of different materials tested for a single aircraft model, and $N_{\text{elem}}$ is the number different types of structural elements tested. In this study, these values are taken as $N_{\text{mat}} = 80$, and $N_{\text{elem}} = 100$, respectively. Note that the cost function in Eq. (11) has the weakness of disregarding the detrimental effects of the failure in tests. The effects include increased product development cycle, delay in production and delivery, and even order cancellation and loss of prestige. Since there are no published data in literature, these effects are not included in the cost function.

The flowchart of the reliability-based design optimization (RBDO) problem is given in Fig. 1. Optimization framework starts with determining the design variables of the problem. Here, the design variables are $(k_f)_W$, $(k_f)_T$, $(n_c)_W$, $(n_c)_T$, $(n_e)_W$, and $(n_e)_T$. Then the lower and upper limits for the design variables are specified in Eq. (1d). Then the objective function and constraints are specified. Here, the objective function is the direct operating cost and the constraint is on the probability of failure of the wing and the tail system. The evaluations of the load-carrying areas and the probability of failure of the wing and tail system are computationally expensive. Therefore, response-surface models are constructed for these responses. For that purpose, first training points are generated in the design variable space using design of experiments methodology. Then the responses (load-carrying areas and the system probability of failure) are computed at the training points. The training points and the corresponding responses constitute the training set. The training set is then used to generate the response-surface approximations. The cost parameters and the constructed response surfaces are used in solving the optimization problem for minimum direct operating cost.

[†]Based on private communications with structural engineers in Turkish Aerospace Industries, Boeing, and NASA.

## III. Assumptions, Simplifications, and Limitations

The major assumptions, simplifications, and limitations of this study can be listed as follows:

1) A representative wing and tail system is considered and the focus is placed on the most critical parts of the wing and tail. It is assumed that each of these critical regions can be characterized by a load-carrying area.

2) The critical regions are assumed to be designed against a static point stress failure. Other failure mechanisms (e.g., fatigue, corrosion, etc.) are not considered.

3) It is assumed that both the wing and the tail structures are stressed equally for the nominal design. The nominal probabilities of failure of the wing and the tail are assumed to be equal.

4) It is assumed that the errors in load calculation for the wing and the tail, and the errors in structural failure assessment for the wing and the tail are perfectly correlated. All other errors and variabilities for the wing and the tail are assumed to be uncorrelated.

5) Safety measures for protection against uncertainties are restricted to the use of a load safety factor and conservative material properties, while other measures such as redundancy are left out.

6) Uncertainty analysis is simplified by classifying uncertainties into two parts: errors and variability. It is very rare to have data on the probability distribution of errors. The errors are assumed to follow uniform probability distribution with known bounds based on experience. The uniform distribution is based on the principle of maximum entropy. The bounds of errors and probability distributions of variabilities are selected based on previous work [17,19,20].

7) Aircraft companies are assumed to follow conservative design practices at each stage of design process. It is assumed that these conservative practices can be simulated by using an additional knockdown factor, $k_f$, over FAA regulations. The nominal value of $k_f$ is taken as 0.95 (for both the wing and tail).

8) It is assumed that a typical airliner has a production line of 1000 aircraft before it is discontinued or substantially redesigned. In addition, 1 out of 1000 aircraft is assumed to experience limit load throughout its service life.

9) The structural test pyramid that has many layers (e.g., coupon tests, element tests, part tests, subassembly tests, assembly tests, and certification test) is simplified to a three-level test pyramid composed of coupon tests, element tests, and certification test only.

10) The nominal value for the material coupon tests (for both the wing and the tail) is assumed to be 50.

11) The nominal value for the structural element tests (for both the wing and the tail) is assumed to be 3.

If these assumptions and simplifications are not valid, then the problem will be complex. For instance, if the optimization was not driven only by the most critical components, then the number of design variables will be increased, thereby larger number of training points will be needed to construct the response-surface models, so the computational cost will be larger. Similarly, if failure mechanisms other than static failure (e.g., fatigue, corrosion, etc.) are considered, then the problem will be more difficult to solve. For the case of fatigue, for instance, a new limit-state function needs to be written for fatigue failure, and reliability calculations for the wing and the tail need to take multiple failure modes into account. This can be achieved through Monte Carlo simulations, but the computational cost will increase. In addition, new design variables such as the number of inspections and types of inspections to be performed need to be introduced, and this will further increase the problem complexity and the computational cost. Another issue is the level of safety. If the reliability level is increased to $10^{-9}$, then Monte Carlo simulation (MCS) will become unaffordable. In that case, instead of MCS method more efficient techniques such as the guided tail modeling method [30] could be used. Nevertheless, the optimization framework demonstrated in Sec. II will still be valid.

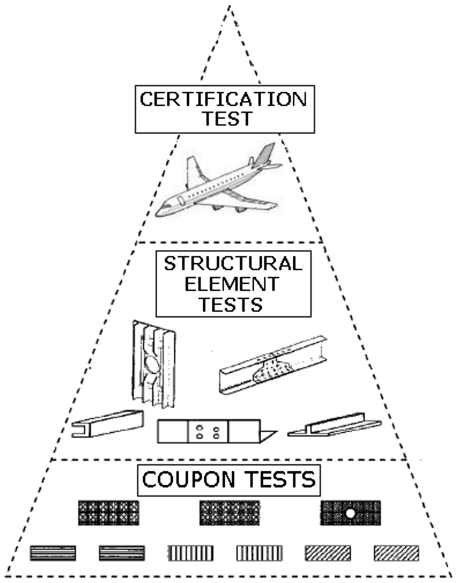


**Fig. 2 Simplified three-level tests.**

## IV. Safety Measures

As noted earlier, the safety of aircraft structures is achieved by designing these structures to operate well in the presence of uncertainties and taking steps to reduce the uncertainties. The following gives brief description of these safety measures.

### A. Safety Measures for Designing Structures Under Uncertainties

In transport aircraft design, FAA regulations mandate the use of a *load safety factor* of 1.5 (FAR 25.303 [31]). That is, aircraft structures are designed to withstand 1.5 times the limit load without failure. Limit load is the maximum load anticipated on the aircraft or component during its service life.

To account for uncertainty in material properties, FAA regulations mandate the use of *conservative material properties* (FAR 25.613 [32]). The conservative material properties are characterized as A-basis and/or B-basis material property values. Detailed information on these values is provided in [33] (Chapter 8). In this paper, B-basis values are used. The B-basis value is determined by calculating the value of a material property exceeded by 90% of the population with 95% confidence. The basis values are determined by testing a number of coupons selected randomly from a material batch. In this paper, the nominal number of coupon tests is taken as 50.

Other safety measures, such as redundancy, are not discussed in this paper.

### B. Safety Measures for Reducing Uncertainties

Improvements in accuracy of structural analysis and failure prediction of aircraft structures reduce errors and enhance the level of safety. These improvements may be due to better modeling techniques developed by researchers, more detailed finite element models made possible by faster computers, or more accurate failure theories. Similarly, the variability in material properties can be reduced through quality control and improved manufacturing processes. Variability reduction in damage and ageing effects is accomplished through inspections and structural health monitoring. The reader is referred to the papers by Qu et al. [15] for effects of variability reduction, Acar et al. [16] for effects of error reduction, and Acar et al. [17] for effects of reduction of both error and variability.

In this paper, the main focus is placed on error reduction through aircraft structural tests, while the other uncertainty-reduction measures are left out for future studies. Structural tests are conducted in a building-block procedure ([33], chapter 2). First, individual coupons are tested to estimate the mean and variability in failure stress. The mean structural failure is estimated based on failure criteria (such as Tsai-Wu) and this estimate is further improved using element tests. Then components, subassemblies, and assemblies are tested, followed by a full-scale test of the entire structure. In this paper, the simplified three-level test procedure depicted in Fig. 2 is used. The coupon tests, structural element tests, and the final certification test are included.

At the first level of testing, coupons (i.e., material samples) are tested to estimate the failure stress. FAR 25.613 [32] mandates aircraft companies to perform enough tests to establish design values of material-strength properties (A-basis or B-basis value). As the number of coupon tests increases, the errors in the assessment of the material properties are reduced. However, since testing is costly, the number of coupon tests is limited to about 100 to 300 for A-basis calculation and at least 30 for B-basis value calculation. In this paper, B-basis values are used and the nominal number of coupon tests is taken as 50.

At the second level of testing, structural elements are tested. The main target of element tests is to reduce errors related to failure theories (e.g., von Mises, Tsai-Wu) used in assessing the failure load of the structural elements. In this paper, the nominal number of structural element tests is taken as 3.

At the uppermost level, certification testing of the overall structure is conducted [Federal Aviation Regulation (FAR) 25.307 [34]]. This final certification testing is intended to reduce the chance of failure in flight due to errors in the structural analysis of the overall structure (e.g., errors in finite element analysis and errors in failure mode prediction). Note that no physical tests have been performed in this work, but the possible tests outcomes are simulated assuming that the probability distribution of the failure stress is known.

## V. Uncertainty Classification, Modeling, and Probability of Failure Calculation

### A. Uncertainty Classification

A good analysis of different sources of uncertainty in engineering simulations is provided by Oberkampf et al. [35,36]. To simplify the analysis, we use a classification that distinguishes between errors (uncertainties that apply equally to the entire fleet of an aircraft model) and variability (uncertainties that vary for the individual aircraft) as used in previous studies [37,38]. The distinction, presented in Table 1, is important because safety measures usually target either errors or variability. While variabilities are random uncertainties that can be readily modeled probabilistically, errors are fixed for a given aircraft model (e.g., Boeing 737-400) but they are largely unknown. Since errors are epistemic, they are often modeled using fuzzy numbers or possibility analysis [39,40]. The errors are modeled probabilistically by using uniform distributions, because

**Table 1 Uncertainty classification**

| Type of uncertainty | Spread | Cause | Remedies |
|---|---|---|---|
| Error (mostly epistemic) | Departure of the average fleet of an aircraft model (e.g., Boeing 737–400) from an ideal | Errors in predicting structural failure, construction errors, deliberate changes | Testing and simulation to improve the mathematical model and the solution |
| Variability (aleatory) | Departure of an individual aircraft from fleet level average | Variability in tooling, manufacturing process, and flying environment | Improvement of tooling and construction; quality control |

these distributions correspond to minimum knowledge or maximum entropy.

### B. Uncertainty Modeling

Detailed discussion on uncertainty modeling can be found in Appendix A. The variabilities in loading, geometry and material properties are modeled with proper probability distributions. The loading is assumed to follow type I extreme distribution, since the maximum load over lifetime is considered. Uniform distribution is used to model uncertainty in geometry. The failure stress is assumed to follow normal distribution.

The errors in load calculation, structural analysis, geometric properties, and failure stress are also modeled. To model the errors related to the failure stress, it is required to simulate the coupon tests, the element tests, and the certification test. At the coupon level, there exist errors in estimating material-strength properties from coupon tests, due to the limited number of coupon tests. At the element level, there exist errors in structural element strength predictions due to the inaccuracy of the failure criterion used. The effects of structural element tests are considered by using Bayesian updating. Discussion on Bayesian updating of the failure stress distribution using the results of element tests is provided in Appendix B. At the certification level, there exist errors in failure prediction of the overall structure.

After all the errors and variability are carefully introduced, the simulation of error and variability can be easily implemented through separable MCS framework [37]. The details of the separable MCS method can be found in Appendix C.

### C. Probability of Failure Calculation for Wing and Tail

As noted earlier, the effect of element tests on failure stress distribution is modeled using Bayesian updating. If Bayesian updating were used directly within an MCS loop of probability of failure calculation, the computational cost would be very high. Therefore, Bayesian updating is performed aside in a separate MCS (a brief description of the procedure is given in Fig. 3 with an illustrative example), before starting with the main MCS loop (a brief sketch of the procedure is provided in Table 2). Since the failure stress distribution may have a general shape, Johnson distribution is used to model it, which can be represented using four quantiles. The procedure followed for Bayesian updating can be described briefly as follows. First, the four quantiles of the mean failure stress are modeled as normal distributions. Then these quantiles are used to fit a Johnson distribution to the mean failure stress. Finally, Bayesian updating is used to update the mean failure stress distribution as in our earlier work [24].

In the main MCS loop, first the coupon tests are simulated and the B-basis allowable stress is calculated. Using the B-basis value, a load-carrying area is computed. Then the effect of structural elements tests is considered (using the Bayesian updating procedure explained above), and the precalculated quantiles of the updated mean failure stress is used. After that, B-basis allowable stress at the element level is calculated. Comparing the B-basis values computed at the coupon level and element level, the load-carrying area values are revised. Finally, using the revised areas, the probability of failure for the wing and the tail, $P_{fW}$ and $P_{fT}$, are computed. 100,000 samples are used in the separable MCS.

### D. System Probability of Failure Calculation

Recall that a representative wing and tail system is considered in this study. It is assumed that the errors in load calculation for the wing and the tail, and the errors in structural failure assessment for the wing and the tail are perfectly correlated. All other errors and variabilities for the wing and the tail are assumed to be uncorrelated. The

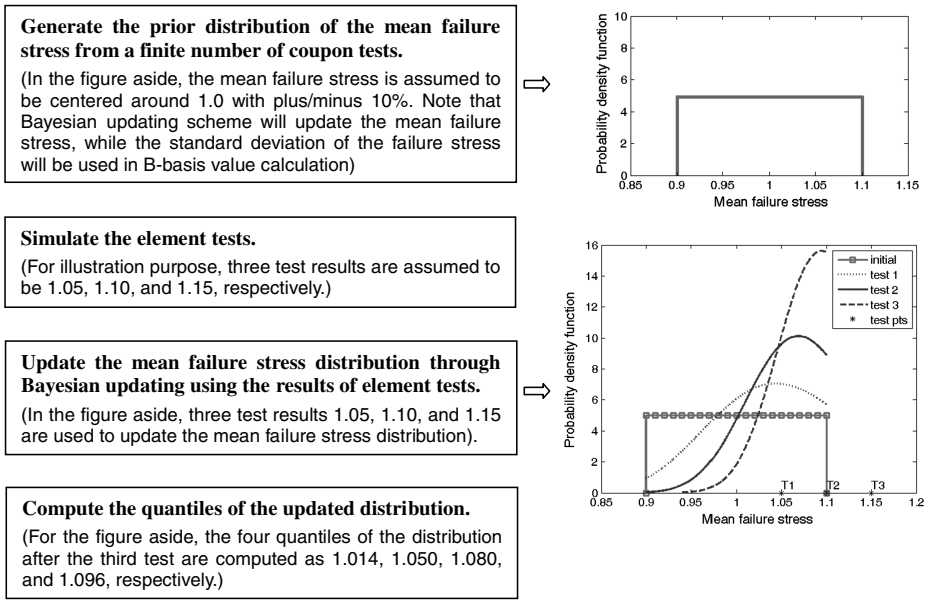


The steps above are repeated for 20,000 times, and the mean and standard deviation as well as the correlation coefficient between the quantiles are computed. Note that for the illustrative example, the four quantiles of the initial distributions are 0.913, 0.962, 1.038, and 1.087, respectively. Since the test results are all conservative, the four quantiles are increased to the larger values 1.014, 1.050, 1.080, and 1.096, respectively.

**Fig. 3 Illustration of the Bayesian updating scheme to update the mean failure stress distribution.**

**Table 2 Monte Carlo procedure for the main code (computing probability of failure of the wing and the tail)**

1) Compute the B-basis allowable stress based on the results of coupon tests.
2) Calculate the average load-carrying area using the results of coupon tests (see Appendix A).
3) Generate random quantiles for the updated mean failure stress (updating was performed in a separate Bayesian updating code, see Fig. 3).
4) Calculate the B-basis allowable stress at the element level using the quantiles (see Appendix B).
5) Revise the load-carrying area based on the values of the B-basis values calculated from the coupon tests (step 1), and element tests (step 4).
6) Using the revised area, compute the probability of failure for wing and tail (see Appendix C), and the correlation coefficient between the revised areas of the wing and the tail.

**Table 3 Evaluating accuracies of response-surface models using leave-one-out cross-validation errors**

| Response | Mean of response | RMSE | MAE | MAXE |
|---|---|---|---|---|
| $A_W$ | 1.31 | 0.002 | 0.001 | 0.006 |
| $A_T$ | 1.31 | 0.002 | 0.001 | 0.005 |
| Rel. index, $\beta_S$ | 5.26 | 0.015 | 0.012 | 0.057 |

correlation coefficient between the load-carrying areas of the wing and the tail is computed within the separable MCS framework, and used in the system reliability calculation that discussed in detail next. Note that the correlation coefficient for the nominal case is computed as 0.752.

The failure probabilities of the wing and the tail are denoted by $P_{fW}$ and $P_{fT}$, and the corresponding reliability indices are denoted by $\beta_W$ and $\beta_T$, respectively. To compute the system failure probability, first the probability of simultaneous failure of the wing and the tail $(P_f)_{W\&T}$ is computed. To simplify the computation, it is assumed that marginal distributions of the limit-state functions for the wing and the tail are normal. Then the probability of simultaneous failure of the wing and the tail is easily computed from [41]

$$(P_f)_{W\&T} = P_{fW}P_{fT} + \int_0^{\rho} \varphi_2(-\beta_W, -\beta_T; \rho)\, \mathrm{d}\rho \tag{12}$$

where $\rho$ is the correlation coefficient, $\varphi_2(\cdot)$ is the bivariate joint probability density function of the standard normal distribution. Finally, since the wing and tail system is a series system, the system failure probability is computed from

$$P_{\mathrm{FS}} = P_{fW} + P_{fT} - (P_f)_{W\&T} \tag{13}$$

## VI. Results

In this section, first the details of response-surface construction for the load-carrying areas and the system reliability index in terms of design variables are presented. Then the reliability-based design optimization of the wing and tail system together with the number of their structural tests is performed for minimum direct operating cost. The optimal number of tests and knockdown factors for the wing and the tail are computed.

### A. Response-Surface Generation for Load-Carrying Area and Reliability Index

Response-surface models (quadratic polynomial with all terms included) are constructed to relate the number of structural tests, additional company knockdown factors to structural weight, and structural safety to be used in the optimization. Overall 100 training points are generated [within the bounds given in Eq. (1d)] using the Latin hypercube sampling design of experiments. The load-carrying areas of the wing $A_W$ and tail $A_T$ (surrogates for the structural weights) and the system reliability index $\beta_S$ (surrogate for the system probability of failure) are computed using separable Monte Carlo simulations, as discussed earlier. The accuracies of the constructed response-surface models are evaluated by using leave-one-out cross-validation errors. That is, response-surface models are constructed 100 times, each time leaving out one of the training points. The difference between the exact response at the omitted point and that predicted by each variant response-surface model defines the cross-validation error. Table 3 provides the root-mean-square error (RMSE), the mean absolute error (MAE), the maximum absolute error (MAXE), and the mean of the response. Comparison of the error metrics with the mean of response reveals that the constructed response surfaces are quite accurate. Note also that the correlation coefficients computed for the 100 training points ranged between 0.620 and 0.808.

### B. RBDO of the Representative System for Minimum Cost

Using the response-surface models constructed, the RBDO problem stated in Eq. (1) is solved by using `fmincon` function of MATLAB® based on the sequential quadratic programming algorithm. To increase the chance of finding the global optimum, multiple starting point strategy is used. The solution of the optimization problem yields real numbers for the number of tests, but they should be integer numbers. To resolve this issue, the following approach is followed. After the optimum solution is obtained as real numbers for the design variables, the numbers of coupon tests for the wing and the tail are rounded to the nearest integers. For instance, if the optimum values are found as $(n_c)_W = 70.71$ and $(n_c)_T = 60.15$, then they are rounded to $(n_c)_W = 71$ and $(n_c)_T = 60$, respectively. For the numbers of element tests, on the other hand, the nearest two integers are considered, which yields four combinations. For instance, if the optimum numbers of element tests for the wing and the tail are found as $(n_e)_W = 3.71$ and $(n_e)_T = 2.15$, respectively, then the following four $[(n_e)_W, (n_e)_T]$ combinations are considered: (3, 2), (4, 2), (3, 3), and (4, 3). Then for each of these combinations, the optimization problem in Eq. (1) is reduced to a two-variable optimization problem

**Table 4 RBDO results when $p = 100$/lb**

| | $k_f$ | $n_c$ | $n_e$ | Weight,[a] lb | $P_f$, $10^{-7}$ | $p^W$, \$M | $C_c$, \$M | $C_e$, \$M | DOC, [b]\$M |
|---|---|---|---|---|---|---|---|---|---|
| *Nominal values* | | | | | | | | | |
| Wing | 0.95 | 50 | 3 | 30,000 | 0.745 | 3,000 | 1.2 | 45 | 3,046.2 |
| Tail | 0.95 | 50 | 3 | 6,000 | 0.745 | 600 | 1.2 | 45 | 646.2 |
| System | —— | —— | —— | 36,000 | 1.471 | 3,600 | 2.4 | 90 | 3,692.4 |
| *Optimum values* | | | | | | | | | |
| Wing | 0.9692 | 80 | 3 | 29,206 | 1.251 | 2,920.6 | 1.9 | 45 | 2,967.5 |
| Tail | 0.8831 | 100 | 1 | 6,405 | 0.242 | 640.5 | 2.4 | 15 | 657.9 |
| System | —— | —— | —— | 35,611 | 1.471 | 3,561.1 | 4.3 | 60 | 3,625.4 |

[a]Overall weight savings ≈389 lb (per airplane).
[b]Overall cost savings ≈67 million.

**Table 5 RBDO results when $p = 200$/lb**

| | $k_f$ | $n_c$ | $n_e$ | Weight,[a] lb | $P_f$, $10^{-7}$ | $p^W$, \$M | $C_c$, \$M | $C_e$, \$M | DOC,[b] \$M |
|---|---|---|---|---|---|---|---|---|---|
| | | | | *Nominal values* | | | | | |
| Wing | 0.95 | 50 | 3 | 30,000 | 0.745 | 6,000 | 1.2 | 45 | 6,046.2 |
| Tail | 0.95 | 50 | 3 | 6,000 | 0.745 | 1,200 | 1.2 | 45 | 1,246.2 |
| System | —— | —— | —— | 36,000 | 1.471 | 7,200 | 2.4 | 90 | 7,292.4 |
| | | | | *Optimum values* | | | | | |
| Wing | 0.9731 | 77 | 3 | 29,088 | 1.378 | 5,817.5 | 1.8 | 45 | 5,864.3 |
| Tail | 0.8901 | 100 | 3 | 6,328 | 0.227 | 1,265.6 | 2.4 | 45 | 1,313.0 |
| System | —— | —— | —— | 35,416 | 1.471 | 7,083.1 | 4.2 | 90 | 7,177.3 |

[a]Overall weight savings ≈584 lb (per airplane).
[b]Overall cost savings ≈115 million.

**Table 6 RBDO results when $p = 300$/lb**

| | $k_f$ | $n_c$ | $n_e$ | Weight,[a] lb | $P_f$, $10^{-7}$ | $p^W$, \$M | $C_c$, \$M | $C_e$, \$M | DOC,[b] \$M |
|---|---|---|---|---|---|---|---|---|---|
| | | | | *Nominal values* | | | | | |
| Wing | 0.95 | 50 | 3 | 30,000 | 0.745 | 9,000 | 1.2 | 45 | 9,046.2 |
| Tail | 0.95 | 50 | 3 | 6,000 | 0.745 | 1,800 | 1.2 | 45 | 1,846.2 |
| System | —— | —— | —— | 36,000 | 1.471 | 10,800 | 2.4 | 90 | 10,892.4 |
| | | | | *Optimum values* | | | | | |
| Wing | 0.9748 | 76 | 4 | 29,008 | 1.376 | 8,702.4 | 1.8 | 60 | 8,764.2 |
| Tail | 0.8894 | 100 | 3 | 6,333 | 0.225 | 1,899.9 | 2.4 | 45 | 1,947.3 |
| System | —— | —— | —— | 35,341 | 1.471 | 10,602.3 | 4.2 | 105 | 10,711.5 |

[a]Overall weight savings ≈659 lb (per airplane).
[b]Overall cost savings ≈181 million.

**Table 7 RBDO results when $p = 500$/lb**

| | $k_f$ | $n_c$ | $n_e$ | Weight,[a] lb | $P_f$, $10^{-7}$ | $p^W$, \$M | $C_c$, \$M | $C_e$, \$M | DOC,[b] \$M |
|---|---|---|---|---|---|---|---|---|---|
| | | | | *Nominal values* | | | | | |
| Wing | 0.95 | 50 | 3 | 30,000 | 0.745 | 15,000 | 1.2 | 45 | 15,046.2 |
| Tail | 0.95 | 50 | 3 | 6,000 | 0.745 | 3,000 | 1.2 | 45 | 3,046.2 |
| System | —— | —— | —— | 36,000 | 1.471 | 18,000 | 2.4 | 90 | 18,092.4 |
| | | | | *Optimum values* | | | | | |
| Wing | 0.9756 | 75 | 4 | 28,992 | 1.394 | 14,495.9 | 1.8 | 60 | 14,557.7 |
| Tail | 0.8918 | 100 | 4 | 6,309 | 0.227 | 3,154.3 | 2.4 | 60 | 3,216.7 |
| System | —— | —— | —— | 35,301 | 1.471 | 17,650.2 | 4.2 | 120 | 17,774.4 |

[a]Overall weight savings ≈699 lb (per airplane).
[b]Overall cost savings ≈318 million.

[in terms of $(k_f)_W$ and $(k_f)_T$ only], and the optimum values of $(k_f)_W$ and $(k_f)_T$ are calculated. Finally, the combination with the best performance (i.e., with minimum direct operating cost) is declared as the optimum.

The RBDO results for $p = 100$/lb are provided in Table 4. The optimum number of coupon tests for the wing and the tail are found as $(n_c)_W = 80$ and $(n_c)_T = 100$, respectively. The optimum number of element tests for the wing and the tail are found as $(n_e)_W = 3$ and $(n_e)_T = 1$, respectively. Table 4 shows that 405 lb of the wing material (about 1.4% of the wing material) is moved to the tail. This operation reduces the reliability of the wing and increases the reliability of the tail, while the system reliability is maintained. The optimization results in an overall weight savings of 389 lb (per airplane) and an overall cost savings of \$67 million (for the entire fleet with $N_a = 1000$ airplanes).

The RBDO results corresponding to the penalty parameters $p = 200$/lb, 300/lb, 500/lb, and 1000/lb are provided in Tables 5–8, respectively. In addition, the summary of RBDO results for various penalty-parameter values is given in Table 9, and the graphical depictions of these results are provided in Fig. 4. The variation of the optimum number of coupon tests and element tests as well as the optimum values of the knockdown factors for the wing and the tail are

**Table 8 RBDO results when $p = 1000$/lb**

| | $k_f$ | $n_c$ | $n_e$ | Weight,[a] lb | $P_f$, $10^{-7}$ | $p^W$, \$M | $C_c$, \$M | $C_e$, \$M | DOC,[b] \$M |
|---|---|---|---|---|---|---|---|---|---|
| | | | | *Nominal values* | | | | | |
| Wing | 0.95 | 50 | 3 | 30,000 | 0.745 | 30,000 | 1.2 | 45 | 30,046.2 |
| Tail | 0.95 | 50 | 3 | 6,000 | 0.745 | 6,000 | 1.2 | 45 | 6,046.2 |
| System | —— | —— | —— | 36,000 | 1.471 | 36,000 | 2.4 | 90 | 36,092.4 |
| | | | | *Optimum values* | | | | | |
| Wing | 0.9756 | 75 | 4 | 28,992 | 1.394 | 28,991.8 | 1.8 | 60 | 29,053.6 |
| Tail | 0.8918 | 100 | 4 | 6,309 | 0.227 | 6,308.7 | 2.4 | 60 | 6,371.1 |
| System | —— | —— | —— | 35,301 | 1.471 | 35,300.5 | 4.2 | 120 | 35,424.7 |

[a]Overall weight savings ≈699 lb (per airplane).
[b]Overall cost savings ≈668 million.

**Table 9 Summary of RBDO results for various penalty-parameter values**

| $p$, /lb | $(k_f)_W$ | $(k_f)_T$ | $(n_c)_W$ | $(n_c)_T$ | $(n_e)_W$ | $(n_e)_T$ | Weight savings, lb | Cost savings, $M |
|---|---|---|---|---|---|---|---|---|
| 100 | 0.969 | 0.883 | 80 | 100 | 3 | 1 | 389 | 67 |
| 200 | 0.973 | 0.890 | 77 | 100 | 3 | 3 | 584 | 115 |
| 300 | 0.975 | 0.889 | 76 | 100 | 4 | 3 | 659 | 181 |
| 500 | 0.976 | 0.892 | 75 | 100 | 4 | 4 | 699 | 318 |
| 1000 | 0.976 | 0.892 | 75 | 100 | 4 | 4 | 699 | 668 |

depicted in Figs. 4a–4c, and the overall cost savings with respect to the weight penalty parameter is shown in Fig. 4d.

The general observations obtained from the RBDO results given in Tables 4–9 and Fig. 4 can be summarized as follows:

1) The optimum reliability allocation for minimum cost is obtained by moving a small fraction of the wing material to the tail. This operation increases the wing failure probability, decreases the tail failure probability while the system reliability is maintained. The optimum value of the probability of failure of the wing is larger than that of the tail.

2) Since the wing material is moved to the tail during optimization, the optimum company knockdown factor for the wing is larger (i.e., the safety factor is smaller) than that of the tail.

3) Since the probability of failure of the wing is larger than that of the wing, the optimum number of element tests for the wing is larger than or equal to that of the tail to compensate for that.

4) The optimum number of coupon tests for the wing is smaller than the tail, and they are almost independent of the weight penalty parameter. The optimum number of coupon tests for the wing is around 75 to 80 and for the tail 100.

5) As the weight penalty parameter $p$ increases, the economical value of the structural weight increases; hence, the structural weight reduction of the system and the overall cost savings increase.

## VII. Conclusions

In most RBDO studies, only the variables that are available at the design stage is considered. Recently, a new reliability-based design framework that can include both predesign and postdesign uncertainty-reduction variables has been proposed. The present study elaborates on that by taking a first step toward performing system reliability-based aircraft structural design together with tests.

In this paper, a representative wing and tail system was considered and sizing optimization of the system based on the design of the most critical components of the wing and the tail was performed. The wing and tail system was designed together with the corresponding number of structural tests for the wing and the tail. The number of coupon tests and the number of structural element tests to be performed for the wing and the tail as well as the additional company knockdown factors for the wing and the tail are selected as design variables to perform system reliability-based optimization for minimum direct operating cost.

The solution of the reliability-based optimization problem revealed that the direct operating cost of the system could be reduced (without sacrificing the overall system safety) by moving a fraction of the material of the wing to the tail. This operation led to reduced safety of the wing and increased safety of the tail, while the system safety was maintained. Consequently, the optimum company

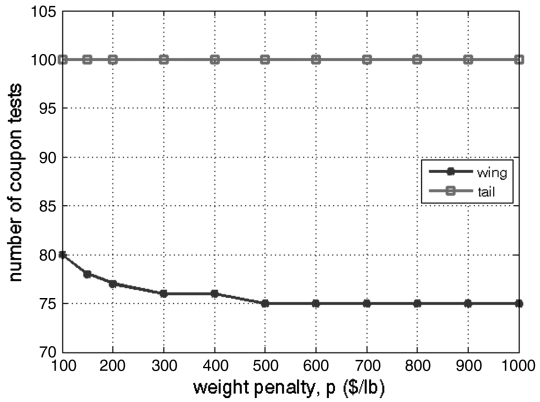


a) The optimum number of coupon tests

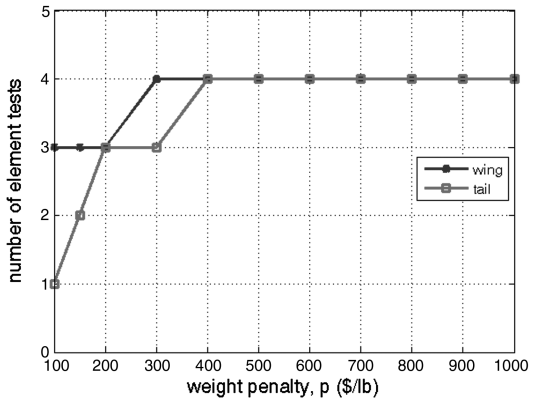


b) The optimum number of element tests

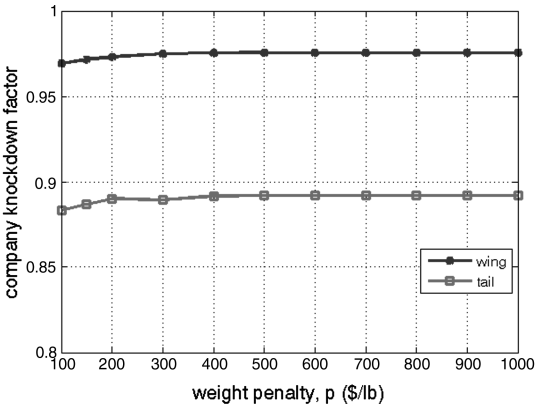


c) The optimum company knockdown factor

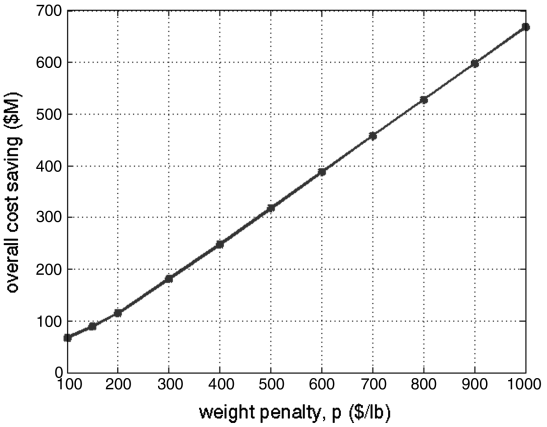


d) The overall cost saving

**Fig. 4 Variation of the optimum number of coupon tests, the optimum number of element tests, the optimum knockdown factor and the overall cost savings with the weight parameter $p$.**

knockdown factor for the wing was larger than that of the tail. It was also found that the optimum number of structural element tests for the wing was larger than or equal to that of the tail. In addition, it was found that the optimum number of coupon tests for the wing was smaller than that of the tail.

The current structural design practices for the wing and the tail do not differ much in terms of the number of tests and the additional company knockdown factors used. That is, the same number of tests is conducted for the structural elements of the wing and the tail. Similarly, the degree of conservatism in the wing structural design and the tail structural design are the same. The results of this study, on the other hand, showed that the wing can be designed with less conservative practices but a larger number of structural element tests, compared with the tail. This approach will lead to a lighter wing and a heavier tail with lighter aircraft overall having the same system reliability.

## Appendix A: Details of Modeling Errors and Variability

### I. Errors in Estimating Material-Strength Properties from Coupon Testing

Coupon tests are conducted to obtain the statistical characterization of material-strength properties, such as failure stress, and their corresponding design values (A-basis or B-basis). With a finite number $n_c$ of coupon tests, the statistical characterization involves errors. Therefore, the calculated values of the mean and the standard deviation of the failure stress will be uncertain. We assume that the failure stress follows normal distribution, so the calculated mean also follows normal distribution. In addition, when $n_c$ is larger than 25, the distribution of the calculated standard deviation tends to be normal. Then the calculated failure stress can be expressed as

$$(\sigma_{cf})_{\text{calc}} = \text{Normal}[(\bar{\sigma}_{cf})_{\text{calc}}; \text{Std}(\sigma_{cf})_{\text{calc}}] \tag{A1}$$

where calculated mean and the calculated apparent standard deviation can be expressed as

$$(\bar{\sigma}_{cf})_{\text{calc}} = \text{Normal}\left(\bar{\sigma}_f; \frac{\text{Std}(\sigma_f)}{\sqrt{nc}}\right) \tag{A2}$$

$$\text{Std}(\sigma_{cf})_{\text{calc}} = \text{Normal}\left(\text{Std}(\sigma_f)\sqrt{\frac{1+\sqrt{\frac{n_c-3}{n_c-1}}}{2}}; \text{Std}(\sigma_f)\sqrt{\frac{1-\sqrt{\frac{n_c-3}{n_c-1}}}{2}}\right) \tag{A3}$$

where $\bar{\sigma}_f$ and $\text{Std}(\sigma_f)$ are, respectively, the true values of the mean and standard deviation of failure stress. Note that Eqs. (A1–A3) describe a random variable coming from a distribution (normal) whose parameters are also random.

The allowable stress at the coupon level, $\sigma_{ca}$, is computed from the failure stress calculated at the coupon level, $(\bar{\sigma}_{cf})_{\text{calc}}$, by using a knockdown factor $k_d$ as

$$\sigma_{ca} = k_d(\bar{\sigma}_{cf})_{\text{calc}} \tag{A4}$$

The knockdown factor $k_d$ is specified by the FAA regulations (Federal Aviation Regulations). For instance, for the B-basis value of the failure stress, 90% of the failure stresses (measured in coupon tests) must exceed the allowable stress with 95% confidence. The requirement of 90% probability and 95% confidence is responsible for the knockdown factor $k_d$ in Eq. (A4). For normal distribution, the knockdown factor depends on the number coupon tests and the coefficient of variation (COV) of the failure stress as

$$k_d = 1 - k_B(c_{cf})_{\text{calc}} \tag{A5}$$

where $(c_{cf})_{\text{calc}}$ is the COV of failure stress calculated from coupon tests, and $k_B$ is called the tolerance limit factor [33]. The tolerance limit factor $k_B$ is a function of the number of coupon tests $n_c$ as given in [33] (Chapter 8, page 84) as

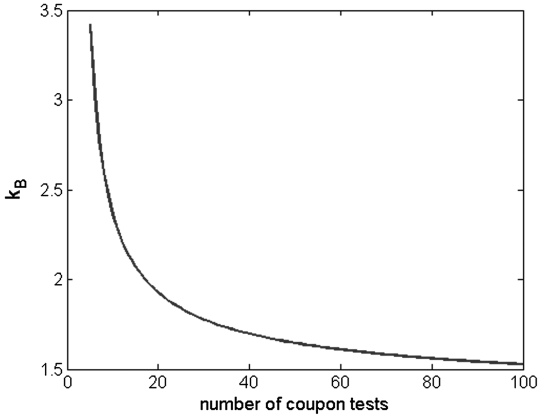


**Fig. A1 Variation of the tolerance coefficient with the number of coupon tests.**

$$k_B \approx 1.282 + \exp\left(0.958 - 0.520\,\ell n(n_c) + \frac{3.19}{n_c}\right) \tag{A6}$$

The variation of the tolerance coefficient with the number of coupon tests is depicted in Fig. A1. Note that Eq. (A6) is valid for normal distribution.

### II. Errors in Structural Element Strength Predictions

The second level in the testing sequence is structural element testing, where structural elements are tested to validate the accuracy of the failure criterion used. Here, we assume that structural element tests are conducted for a specified combination of loads corresponding to critical loading. For this load combination, the failure surface can be boiled down to a single failure stress $\bar{\sigma}_{ef}$, where the subscript $e$ stands for structural element tests. The mean failure stress of the elements $(\bar{\sigma}_{ef})_{\text{calc}}$ can be predicted from the mean failure stress of the coupons $(\bar{\sigma}_{cf})_{\text{calc}}$ through

$$(\bar{\sigma}_{ef})_{\text{calc}} = (1 - e_{ef})(\bar{\sigma}_{cf})_{\text{calc}} \tag{A7}$$

where $e_{ef}$ is the error in the failure theory used. Note that the sign in front of the error term is negative, since we consistently formulate the error expressions such that a positive error implies a conservative decision. The initial distribution of $(\bar{\sigma}_{ef})_{\text{calc}}$ is obtained by estimate of $e_{ef}$ and using the results of coupon tests $(\bar{\sigma}_{cf})_{\text{calc}}$. The information from element tests is used by performing a Bayesian procedure to update the failure stress distribution (see Appendix B for details). In practice, simpler procedures are often used, such as selecting the lowest failure stress from element tests. Therefore, our assumption will tend to overestimate the beneficial effect of element tests.

If Bayesian updating were used directly within the main MCS loop for design load-carrying area determination, the computational cost would be very high. Instead, Bayesian updating is performed outside from the MCS loop for a range of possible test results. It is important to note that the error definition used in the Bayesian updating code is different from the error definition used in the MCS code. In the Bayesian updating code, the error is measured from the calculated values of the failure stress,$(\bar{\sigma}_{ef})_{\text{calc}}$, such that the true and the calculated values of the failure stress are related through $(\bar{\sigma}_{ef})_{\text{true}} = (1 + \text{error})(\bar{\sigma}_{ef})_{\text{calc}}$. In the MCS code, on the other hand, the error is measured from the true value of the failure stress such that the true and the calculated values of the failure stress are related through $(\bar{\sigma}_{ef})_{\text{calc}} = (1 - e_{ef})(\bar{\sigma}_{ef})_{\text{true}}$. Therefore, while the Bayesian updating is implemented, a random error $e_f$ generated in the main MCS code is transferred to error $= [1/(1 - e_{ef})] - 1$ while running the Bayesian updating code. This complication reflects the fact that in the MCS loop we consider many possible element analysis and test results, while the engineer carrying the element tests has a unique set of computations and test results.

The allowable stress based on the element test is calculated from

$$\sigma_{ea} = k_d(\bar{\sigma}_{ef})_{\text{calc}} \tag{A8}$$

Here, the updated value of the mean failure stress $(\bar{\sigma}_{ef})_{\text{calc}}^{\text{updated}}$ is used, which corresponds to the most likely value of the mean failure stress [having the maximum probability density function (PDF)].

Combining Eqs. (A4), (A7), and (A8), we have

$$\sigma_{ea} = (1 - e_{ef})\sigma_{ca} \tag{A9}$$

### III. Errors in Structural Strength Predictions

Because of the complexity of the overall structural system, there will be errors in failure prediction of the overall structure that we denote as $e_f$. If we follow the formulation we used in expressing $(\bar{\sigma}_{ef})_{\text{calc}}$ in terms of $(\bar{\sigma}_{cf})_{\text{calc}}$, the calculated mean failure stress of the overall structure, $(\bar{\sigma}_f)_{\text{calc}}$, can be expressed in terms of the calculated mean failure stress of the structural element, $(\bar{\sigma}_{ef})_{\text{calc}}$, through

$$(\bar{\sigma}_f)_{\text{calc}} = (1 - e_f)(\bar{\sigma}_{ef})_{\text{calc}} \tag{A10}$$

The allowable stress at the structural design level, $\sigma_a$, can be related to the allowable stress computed at the element level, $\sigma_{ea}$, through the following relation:

$$\sigma_a = k_f(1 - e_f)\sigma_{ea} \tag{A11}$$

where $k_f$ is an additional knockdown factor used at the structural level as an extra precaution. Here, $k_f$ is taken 0.95. Combining Eqs. (A9) and (A11), we can obtain

$$\sigma_a = (1 - e_{ef})(1 - e_f)k_f\sigma_{ac} \tag{A12}$$

### IV. Errors in Design

Before starting the structural design, aerodynamic analysis needs to be performed to determine the loads acting on the aircraft. However, the calculated design load value, $P_{\text{calc}}$, differs from the actual design load $P_d$ under conditions corresponding to FAA design specifications (e.g., gust-strength specifications). Since each company has different design practices, the error in load calculation, $e_p$, is different from one company to another. The calculated design load $P_{\text{calc}}$ is expressed in terms of the true design load $P_d$ as

$$P_{\text{calc}} = (1 + e_P)P_d \tag{A13}$$

In addition to the error in load calculation, an aircraft company may also make errors in stress calculation. We consider a small region in a structural part, characterized by a thickness $t$ and width $w$, that resists the load in that region. The value of the stress in a structural part calculated by the stress analysis team, $\sigma_{\text{calc}}$, can be expressed in terms of the load values calculated by the load team $P_{\text{calc}}$, the design width $w_{\text{design}}$, and the thickness $t$ of the structural part by introducing the term $e_\sigma$ representing error in the stress analysis:

$$\sigma_{\text{calc}} = (1 + e_\sigma)\frac{P_{\text{calc}}}{w_{\text{design}}t} \tag{A14}$$

In this paper, we assume that the aircraft companies have the capability of predicting the stresses very accurately so that the effect of $e_\sigma$ is negligible and is taken as zero. The calculated stress value is then used by a structural designer to calculate the design thickness $t_{\text{design}}$. That is, the design thickness can be formulated as

$$t_{\text{design}} = \frac{S_F P_{\text{calc}}}{w_{\text{design}}\sigma_a} = \frac{(1 + e_P)}{(1 - e_f)(1 - e_{ef})}\frac{S_F P_d}{w_{\text{design}}k_f\sigma_{ca}} \tag{A15}$$

Then the design value of the load-carrying area can be expressed as

$$A_{\text{design}} = t_{\text{design}}w_{\text{design}} = \frac{(1 + e_P)}{(1 - e_f)(1 - e_{ef})}\frac{S_F P_d}{k_f\sigma_{ca}} \tag{A16}$$

### V. Errors in Construction

In addition to the above errors, there will also be construction errors in the geometric parameters. These construction errors represent the difference between the values of these parameters in an average airplane (fleet average) built by an aircraft company and the design values of these parameters. The error in width, $e_w$, represents the deviation of the design width of the structural part, $w_{\text{design}}$, from the average value of the width of the structural part built by the company, $w_{\text{built-av}}$. Thus,

$$w_{\text{built-av}} = (1 + e_w)w_{\text{design}} \tag{A17}$$

Similarly, the built thickness value will differ from its design value such that

$$t_{\text{built-av}} = (1 + e_t)t_{\text{design}} \tag{A18}$$

Then the built load-carrying area $A_{\text{built-av}}$ can be expressed using the first equality of Eq. (A16) as

$$A_{\text{built-av}} = (1 + e_t)(1 + e_w)A_{\text{design}} \tag{A19}$$

Table A1 presents the statistical properties for the errors, which are modeled with uniform distributions, following the principle of maximum entropy. The bounds of errors are taken from earlier studies [24,38].

### VI. Total Error $e_{\text{total}}$

The expression for the built load-carrying area of a structural part computed based on coupon test results, $A_{\text{built-av-}c}$, can be reformulated by combining Eqs. (A16) and (A19) as

$$A_{\text{built-av-}c} = (1 + e_{\text{total}})\frac{S_F P_d}{k_f\sigma_{ca}} \tag{A20}$$

where

$$e_{\text{total}} = \frac{(1 + e_P)(1 + e_t)(1 + e_w)}{(1 - e_f)(1 - e_{ef})} - 1 \tag{A21}$$

Here, $e_{\text{total}}$ represents the cumulative effect of the individual errors on the load-carrying capacity of the structural part.

### VII. Redesign Based on Element Tests

In addition to updating the failure stress distribution, element tests have an important role of leading to design changes if the design is unsafe or overly conservative. That is, if very large or very small failure stress values are obtained from the element tests, the company may want to increase or reduce the load-carrying area of the elements. There is no published data on redesign practices, and so we used the following approach [24]. We assumed that if the B-basis value obtained after element tests, $\sigma_{ea}$, is more than 5% higher than the B-basis value obtained from coupon tests, $\sigma_{ca}$, then the load-carrying area is reduced by $\sigma_{ca}/\sigma_{ea}$ ratio. If the B-basis value obtained after element tests is more than 2% lower than the B-basis value obtained from coupon tests, the load-carrying area is increased

**Table A1 Distribution of error terms and their bounds**

| Error factors | Distribution type | Mean | Bounds |
|---|---|---|---|
| Error in load calculation $e_P$ | Uniform | 0.0 | ±10% |
| Error in width $e_w$ | Uniform | 0.0 | ±1% |
| Error in thickness $e_t$ | Uniform | 0.0 | ±3% |
| Error in failure prediction $e_f$ | Uniform | 0.0 | ±10% |
| Error in failure prediction $e_{ef}$ | Uniform | 0.0 | ±10% |

by $\sigma_{ca}/\sigma_{ea}$ amount. This lower tolerance reflects the need for safety. Otherwise, no redesign was performed. The built load-carrying area can be revised by multiplying Eq. (A20) by a redesign correction factor $c_r$ as

$$A_{\text{built-av}} = c_r A_{\text{built-av-}c} = (1 + e_{\text{total}}) c_r \frac{S_F P_d}{k_f \sigma_{ca}} \tag{A22}$$

For no redesign,

$$c_r = 1 \tag{A23a}$$

For redesign,

$$c_r = \frac{1.01}{\text{CF}} \tag{A23b}$$

Since redesign requires new elements to be built and tested, it is costly. Therefore, we do not have a redesign over redesigned elements. To protect against uncertainties in the test of the redesigned element we have an additional 1% reduction in the calculated allowable value [see the term 1.01 in Eq. (A23b)].

## VIII. Variability

In the previous sections, we analyzed the different types of errors made in the design and construction stages, representing the differences between the fleet-average values of geometry, material and loading parameters and their corresponding design values. For a given design, these parameters vary from one aircraft to another in the fleet due to variability in tooling, construction, flying environment, etc. For instance, the actual value of the thickness of a structural part, $t_{\text{built-var}}$, is defined in terms of its fleet-average built value, $t_{\text{built-av}}$, by

$$t_{\text{built-var}} = (1 + v_t) t_{\text{built-av}} \tag{A24}$$

We assume that $v_t$ has a uniform distribution with 3% bounds (see Table A2). Then the actual load-carrying area $A_{\text{built-var}}$ can be defined as

$$A_{\text{built-var}} = t_{\text{built-var}} w_{\text{built-var}} = (1 + v_t)(1 + v_w) A_{\text{built-av}} \tag{A25}$$

where $v_w$ represents effect of the variability on the fleet-average built width.

Table A2 presents the assumed distributions for variabilities. The loading is assumed to follow type I asymptotic distribution, since we consider the maximum load over lifetime. We assume that one of the aircraft in the fleet will experience the limit load over its service life. We assume that a typical airliner has a production line of 1000 aircraft. Thus, the distribution parameters of the loading are computed such that the probability of an aircraft experiencing limit load over its service life is equal to 1/1000, and the coefficient of variation of the loading is 10%. Since the loading is normalized with respect to the failure stress, the limit load is equal to $1/S_F = 2/3$ for our problem. The distribution parameters are found as $a = 28.73$ and $b = 0.4263$, when the cumulative distribution function of the type I asymptotic distribution is defined as

$$F_X(x) = \exp\{-\exp[-a(x - b)]\} \tag{A26}$$

## IX. Certification Test

After a structural part has been built with random errors in stress, load, width, allowable stress and thickness, it is loaded with the design axial force of $S_F$ times $P_{\text{calc}}$, and if the stress exceeds the failure stress of the structure $\sigma_f$, then the structure fails and the design is rejected; otherwise it is certified for use. That is, the structural part is certified if the following inequality is satisfied:

$$\sigma - \sigma_f = \frac{S_F P_{\text{calc}}}{(1 + v_t)(1 + v_w) A_{\text{built-av}}} - \sigma_f \le 0 \tag{A27}$$

The representative system passes certification when the most critical structural parts of both the wing and the tail satisfy Eq. (A27). The details of the Monte Carlo procedure are as follows:

1) Compute the allowable stress based on coupon tests, $\sigma_{ca}$.

2) Calculate the built average load-carrying area using the results of coupon tests,

$$A_{\text{built-av-}c} = (1 + e_{\text{total}}) \frac{S_F P_d}{k_f w_{\text{design}}} \frac{1}{\sigma_{ca}}$$

3) Generate random numbers for the quantiles of the updated mean failure stress.

4) Calculate the B-basis value using the quantiles $\sigma_{ea}$.

a) Compute the bounds for mean failure stress:

$$lb = \frac{1 - be_{ef} - 2c_f/\sqrt{n_c}}{(1 - e_{ef})} \qquad ub = \frac{1 + be_{ef} + 2c_f/\sqrt{n_c}}{(1 - e_{ef})}$$

b) Compute the PDF of the mean failure stress using Johnson distribution with quantiles computed in step 3, and select the mean failure stress value with the highest PDF within the bounds as $(\bar{\sigma}_{ef})^{\text{updated}}_{\text{calc}}$.

c) Compute B-basis value $\sigma_{ea} = [1 - k_B (c_{cf})_{\text{calc}}](\bar{\sigma}_{ef})^{\text{updated}}_{\text{calc}}$.

5) Compute a correction factor (CF) for the B-basis value, $\text{CF} = \sigma_{ea}/\sigma_{ca}$. Limit the value of CF to [0.9, 1.1]. That is, if $\text{CF} < 0.9$, then $\text{CF} = 0.9$. If $\text{CF} > 1.1$, then $\text{CF} = 1.1$.

6) Revise the built average load-carrying area based on the value of CF.

a) $\text{CF} < 0.98$, then redesign is needed, we will increase the load-carrying area by CF. Hence, the new load-carrying area is $A_{\text{built-av}} = (1.01/\text{CF}) A_{\text{built-av-}c}$. Here, the factor 1.01 is used to avoid a second redesign of elements.

b) If $0.98 \le \text{CF} \le 1.05$, then no redesign is needed. So the load-carrying area is $A_{\text{built-av}} = A_{\text{built-av-}c}$.

c) If $\text{CF} > 1.05$, then redesign is needed, we will decrease the load-carrying area by CF. Hence, the new load-carrying area is $A_{\text{built-av}} = (1.01/\text{CF}) A_{\text{built-av-}c}$. Here, again the factor 1.01 is used to avoid a second redesign of elements.

7) Using $A_{\text{built-av}}$, compute the probability of failure.

## Appendix B: Bayesian Updating of the Failure Stress Distribution from the Results of Element Tests

The initial distribution of the element failure stress is obtained by using a failure criterion (e.g., Von Mises for metals, Tsai-Wu for composites) using the results of coupon tests. We consider a typical situation relating to updating analytical predictions of strength based on tests. We assume that the analytical prediction of the failure stress of a structural element, $(\sigma_{ef})_{\text{calc}}$, applies to the average failure stress

**Table A2 Distribution of random variables having variability**

| Variables | Distribution type | Mean | Scatter |
|---|---|---|---|
| Actual service load [a] $P_{\text{act}}$ | type I asymptotic | $a = 28.73$ | $b = 0.4263$ |
| Actual built width $w_{\text{built-var}}$ | Uniform | $w_{\text{built-av}}$ | 1% bounds |
| Actual built thickness $t_{\text{built-var}}$ | Uniform | $t_{\text{built-av}}$ | 3% bounds |
| Failure stress $\sigma_f$ | Normal | 1.0 | 8% COV |
| $v_w$ | Uniform | 0 | 1% bounds |
| $v_t$ | Uniform | 0 | 3% bounds |

[a]For the loading, $a$ and $b$ are not the mean and scatter of the distribution.

$(\bar{\sigma}_{ef})_{\text{true}}$ of an infinite number of nominally identical structural elements. The error $e_{ef}$ of our analytical prediction is defined by

$$(\bar{\sigma}_{ef})_{\text{true}} = (1 + e_{ef})(\sigma_{ef})_{\text{calc}} \tag{B1}$$

Here, we assume that the designer can estimate the bounds $b_e$ (possibly conservative) on the magnitude of the error, and we further assume that the errors have a uniform distribution between the bounds. Note here that it is more convenient to define the error to be measured from the calculated values of the failure stress as shown in Fig. B1.

As in our earlier work [23], we neglect the effect of coupon tests and assumed the initial distribution of the mean failure stress $f^{\text{ini}}(\bar{\sigma}_{ef})$ uniform within the bounds $b_e$ as

$$f^{\text{ini}}(\bar{\sigma}_{ef}) = \begin{cases} \frac{1}{2b_e(\sigma_{ef})_{\text{calc}}} & \text{if } \left|\frac{\bar{\sigma}_{ef}}{(\sigma_{ef})_{\text{calc}}} - 1\right| \le b_e \\ 0 & \text{othewise} \end{cases} \tag{B2}$$

Then the distribution of the mean failure stress is updated using the Bayesian updating with a given $(\sigma_f)_{1,\text{test}}$ as

$$f^{\text{upd}}(\bar{\sigma}_{ef}) = \frac{f_{1,\text{test}}(\bar{\sigma}_{ef}) f^{\text{ini}}(\bar{\sigma}_{ef})}{\int_{-\infty}^{\infty} f_{1,\text{test}}(\bar{\sigma}_{ef}) f^{\text{ini}}(\bar{\sigma}_{ef})\, \mathrm{d}\bar{\sigma}_{ef}} \tag{B3}$$

where $f_{1,\text{test}}$ is the likelihood function reflecting possible variability of the first test result $(\sigma_{ef})_{1,\text{test}}$. The likelihood function can be formulated either using Eq. (B4),

$$f_{1,\text{test}}(\bar{\sigma}_{ef}) = \text{Normal}((\sigma_{ef})_{1,\text{test}}; \bar{\sigma}_{ef}, \text{Std}(\sigma_{cf})) \tag{B4}$$

or using Eq. (B5):

$$f_{1,\text{test}}(\bar{\sigma}_{ef}) = \text{Normal}((\sigma_{ef})_{1,\text{test}}; \bar{\sigma}_{ef}, \bar{\sigma}_{ef} c_{cf}) \tag{B5}$$

Note that the standard deviation of the element failure stress $\text{Std}(\sigma_{ef})$ is taken equal to the standard deviation obtained from coupon tests $\text{Std}(\sigma_{cf})$. Here, we do not have a strong preference on Eqs. (B4) and (B5), so we choose to use the second formulation [Eq. (B5)], as in our earlier work [23].

It should be noted that $f_{1,\text{test}}(\bar{\sigma}_{ef})$ is not a probability distribution in $\bar{\sigma}_{ef}$; it is the conditional probability density of obtaining test result $(\sigma_{ef})_{1,\text{test}}$, given that the mean value of the failure stress is $\bar{\sigma}_{ef}$. Subsequent tests are handled by the same equations, using the updated distribution, as the initial one.

Bayesian updating is performed aside from the MCS loop. In this separate loop, we first simulate the coupon tests by drawing random samples for the mean and standard deviation of the calculated failure stress $\bar{\sigma}_{cf}$ and $\text{Std}(\sigma_{cf})$, and thereby $c_{cf}$. Then we simulate $n_e$ number of element tests, $(\sigma_{ef})_{\text{test}}$. The element test results along with the mean and the standard deviation are used to define the likelihood function [Eq. (B5)] in Eq. (B3). The initial distribution $f^{\text{ini}}(\bar{\sigma}_{ef})$ in Eq. (B3) is uniformly distributed within some bounds as given in Eq. (B6):

$$f^{\text{ini}}(\bar{\sigma}_{ef}) = \begin{cases} \frac{1}{2b_e\bar{\sigma}_{cf}} & \text{if } \left|\frac{\bar{\sigma}_{ef}}{\bar{\sigma}_{cf}} - 1\right| \le b_e \\ 0 & \text{otherwise} \end{cases} \tag{B6}$$

We found that applying the error bounds $b_e$ before the Bayesian updating or after the updating do not matter. Applying the error bounds before Bayesian updating means calculating the initial distribution $f^{\text{ini}}(\bar{\sigma}_{ef})$ from Eq. (B6) and then using Eq. (B3). To apply the error bounds after the Bayesian updating, however, we first assume very large error bounds $b_e$, calculate the initial distribution $f^{\text{ini}}(\bar{\sigma}_{ef})$ from Eq. (B6), and apply the error bounds $b_e$ to the distribution obtained using Eq. (B3).

Applying the error bounds after the Bayesian updating is more useful when we want to fit distributions (e.g., Johnson distribution) to the mean failure stress obtained through Bayesian updating. If we apply the error bounds at the beginning, the distribution after Eq. (B3) will be a truncated one and it will be difficult to fit a distribution with good fidelity. However, if we apply the error bounds at the end, the distribution after Eq. (B3) will be a continuous one and we will most likely fit a good distribution.

The overall procedure is as follows. Within an MCS loop, we generate random mean and standard deviation values for the failure stress to be obtained through coupon tests. Then we assume large error bounds to be used in Eq. (B6), simulate element tests and use Eq. (B3) to obtain the distribution of the mean failure stress. Then we compute the four quantiles of the mean failure stress distribution. Finally, we compute the mean and standard deviations of the quantiles and we model these quantiles as normal distributions. Note that the quantiles are the values of failure stress for cumulative distribution function values of [0.067, 0.309, 0.691, 0.933].

The quantiles are functions of the number of coupon tests $n_c$, number of element tests $n_e$, and the error in failure stress prediction $e_{ef}$. At first, we wanted to build response-surface approximations for the mean and standard deviation of the quantiles in terms of $n_c$ and $e_{ef}$ after each element test. So we would have 10 response-surface approximations (five for the mean and five for the standard deviation) in terms of $n_c$ and $e_{ef}$. Our numerical analysis revealed, on the other hand, that $n_c$ do not have a noticeable effect on quantiles (see Tables B1–B3 and Fig. B2), and the effect of the error can be represented by just multiplying the quantiles with $(1 - e_{ef})$ term (see Table B4).

As noted earlier, the quantiles are assumed to have normal distributions. Figure B3 show the histograms of the first and second quantiles of the mean failure stress (for 50 coupon tests after the third element test when $e_{ef} = 0$) obtained through MCS with 20,000

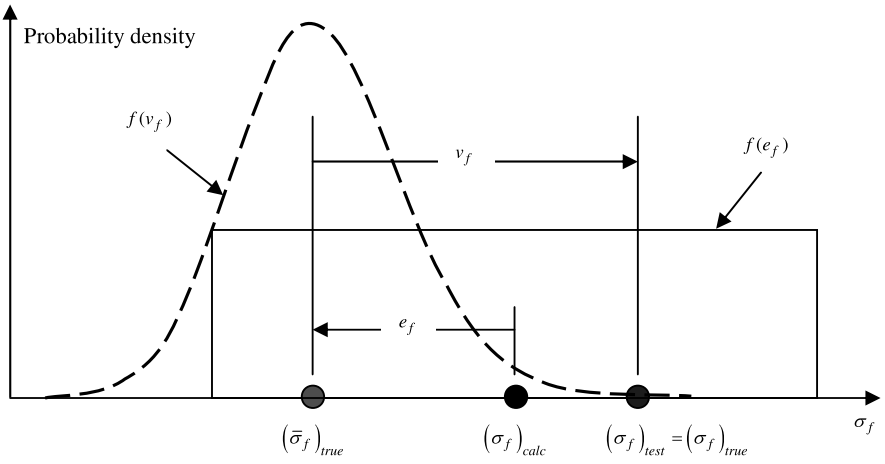


**Fig. B1 Error and variability in failure stress. The error is centered around the computed value, and is assumed to be uniformly distributed here. The variability distribution, on the other hand, is normal with mean equal to the true average failure stress.**

**Table B1 Quantile statistics of mean failure stress after element tests (30 coupon tests)**

| | Mean values of the quantiles ($Q_{1-4}$) | | | | Standard deviation of the quantiles ($Q_{1-4}$) | | | |
|---|---|---|---|---|---|---|---|---|
| | $\bar{Q}_1$ | $\bar{Q}_2$ | $\bar{Q}_3$ | $\bar{Q}_4$ | std ($Q_1$) | std ($Q_2$) | std ($Q_3$) | std ($Q_4$) |
| test1 | 0.899 | 0.968 | 1.049 | 1.145 | 0.073 | 0.077 | 0.084 | 0.094 |
| test2 | 0.925 | 0.975 | 1.032 | 1.096 | 0.053 | 0.055 | 0.058 | 0.063 |
| test3 | 0.937 | 0.979 | 1.025 | 1.076 | 0.044 | 0.045 | 0.047 | 0.051 |
| test4 | 0.945 | 0.982 | 1.021 | 1.065 | 0.038 | 0.039 | 0.041 | 0.043 |
| test5 | 0.950 | 0.983 | 1.019 | 1.057 | 0.035 | 0.036 | 0.037 | 0.039 |

**Table B2 Quantile statistics of mean failure stress after element tests (50 coupon tests)**

| | Mean values of the quantiles ($Q_{1-4}$) | | | | Standard deviation of the quantiles ($Q_{1-4}$) | | | |
|---|---|---|---|---|---|---|---|---|
| | $\bar{Q}_1$ | $\bar{Q}_2$ | $\bar{Q}_3$ | $\bar{Q}_4$ | std ($Q_1$) | std ($Q_2$) | std ($Q_3$) | std ($Q_4$) |
| test1 | 0.897 | 0.966 | 1.047 | 1.143 | 0.073 | 0.078 | 0.084 | 0.093 |
| test2 | 0.924 | 0.975 | 1.032 | 1.095 | 0.053 | 0.055 | 0.058 | 0.063 |
| test3 | 0.937 | 0.979 | 1.025 | 1.075 | 0.044 | 0.045 | 0.047 | 0.050 |
| test4 | 0.944 | 0.981 | 1.021 | 1.064 | 0.038 | 0.039 | 0.041 | 0.043 |
| test5 | 0.950 | 0.983 | 1.019 | 1.057 | 0.035 | 0.035 | 0.037 | 0.039 |

**Table B3 Quantile statistics of mean failure stress after element tests (80 coupon tests)**

| | Mean values of the quantiles ($Q_{1-4}$) | | | | Standard deviation of the quantiles ($Q_{1-4}$) | | | |
|---|---|---|---|---|---|---|---|---|
| | $\bar{Q}_1$ | $\bar{Q}_2$ | $\bar{Q}_3$ | $\bar{Q}_4$ | Std ($Q_1$) | Std ($Q_2$) | Std ($Q_3$) | Std ($Q_4$) |
| test1 | 0.898 | 0.967 | 1.049 | 1.144 | 0.071 | 0.076 | 0.083 | 0.091 |
| test2 | 0.924 | 0.975 | 1.032 | 1.096 | 0.052 | 0.055 | 0.058 | 0.062 |
| test3 | 0.937 | 0.979 | 1.025 | 1.076 | 0.043 | 0.045 | 0.047 | 0.050 |
| test4 | 0.944 | 0.982 | 1.021 | 1.065 | 0.038 | 0.039 | 0.040 | 0.042 |
| test5 | 0.950 | 0.983 | 1.019 | 1.057 | 0.034 | 0.035 | 0.036 | 0.038 |

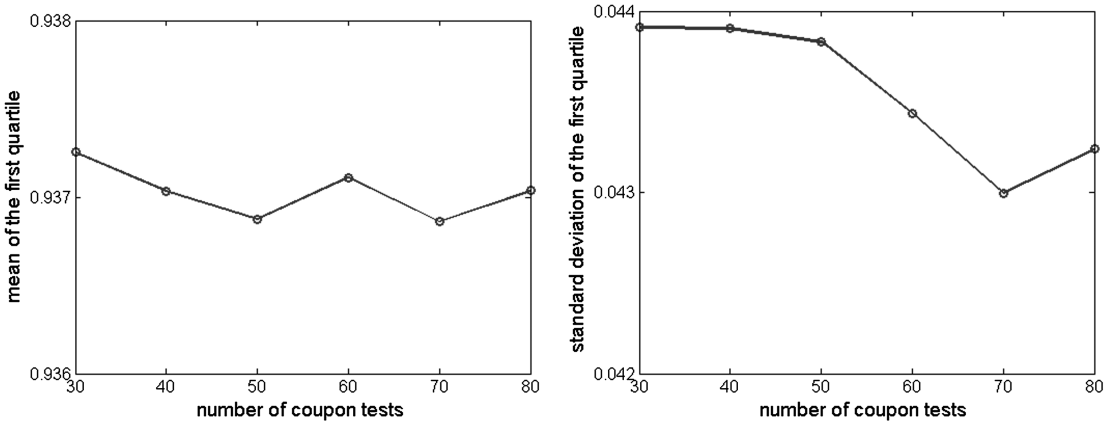


**a) Mean value of the first quantile** **b) Standard deviation of the first quantile**

**Fig. B2 Variation of the mean and standard deviation of the first quartile of the mean failure stress with number of coupon tests (after the third element test).**

**Table B4 Effect of $e_{ef}$ on quantile statistics of mean failure stress**

| | Mean values of the quantiles ($Q_{1-4}$) | | | | Standard deviation of the quantiles ($Q_{1-4}$) | | | |
|---|---|---|---|---|---|---|---|---|
| $e_{ef}$ | $\bar{Q}_1$ | $\bar{Q}_2$ | $\bar{Q}_3$ | $\bar{Q}_4$ | Std ($Q_1$) | Std ($Q_2$) | Std ($Q_3$) | Std ($Q_4$) |
| −0.10 | 0.835 | 0.881 | 0.923 | 0.968 | 0.039 | 0.041 | 0.043 | 0.045 |
| −0.05 | 0.890 | 0.930 | 0.974 | 1.022 | 0.042 | 0.043 | 0.045 | 0.048 |
| 0 | 0.937 | 0.979 | 1.025 | 1.076 | 0.044 | 0.045 | 0.047 | 0.050 |
| 0.05 | 0.983 | 1.027 | 1.075 | 1.128 | 0.045 | 0.047 | 0.049 | 0.052 |
| 0.10 | 1.031 | 1.077 | 1.128 | 1.183 | 0.048 | 0.050 | 0.052 | 0.055 |

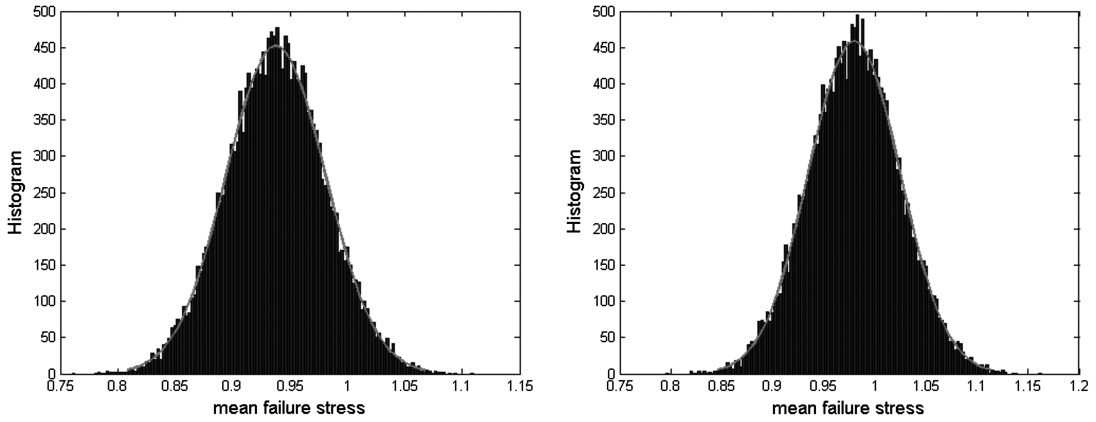


a) Histogram of the first quantile b) Histogram of the second quantile

**Fig. B3 Histograms of the first and the second quantiles of the mean failure stress (after the third element test). The continuous lines show the normal fits.**

samples. We see that the quantiles do not exactly follow normal distributions.

The results obtained in this separate MCS loop are used in the main MCS loop for determining the built average load-carrying area. The mean and standard deviations of the quantiles are used to fit a Johnson distribution to the mean failure stress. The error bounds are then applied to the Johnson distribution and random values from this distribution are drawn whenever element tests are simulated. Note also that the quantiles are strongly correlated to each other, so this correlation is also included in our analysis while random quantiles are generated in the main MCS loop using Gaussian copula. The reader is referred to the work of Noh et al. [42] for further details of reliability estimation of problems with correlated input variables using a Gaussian copula.

## Appendix C: Separable Monte Carlo Simulations

The prediction of probability of failure using conventional MCS requires trillions of simulations for level of $10^{-7}$ failure probability. To address the computational burden, separable Monte Carlo procedure can be used. The reader is referred to Smarslok et al. [43] for more information on the separable Monte Carlo procedure. This procedure applies when the failure condition can be expressed as $g_1(x_1) > g_2(x_2)$, where $x_1$ and $x_2$ are two disjoint sets of random variables. To take advantage of this procedure, we need to formulate the failure condition in a separable form, so that $g_1$ will depend only on variabilities and $g_2$ only on errors. The common formulation of the structural failure condition is in the form of a stress exceeding the material limit. This form does not satisfy the separability requirement, however. For example, the stress depends on variability in material properties as well as design area, which reflects errors in the analysis process. To bring the failure condition to the right form, we instead formulate it as the required cross-sectional area $A'_{\text{req}}$ being larger than the built area $A_{\text{built-av}}$. So the failure condition can be defined in terms of the built area and the required area as

$$A_{\text{built-av}} < \frac{A_{\text{req}}}{(1+v_t)(1+v_w)} \equiv A'_{\text{req}} \tag{C1}$$

where $A_{\text{req}}$ is the cross-sectional area required to carry the actual loading conditions for a particular copy of an aircraft model, and $A'_{\text{req}}$ is what the built area (fleet average) needs to be in order for the particular copy to have the required area after allowing for variability in width and thickness:

$$A_{\text{req}} = P_{\text{act}}/\sigma_f \tag{C2}$$

The required area depends only on variability, while the built area depends only on errors. When certification testing is taken into account, the built area $A_{\text{built-av}}$ is replaced by the certified area $A_{\text{cert}}$, which is the same as the built area for companies that pass certification. However, companies that fail are not included. That is, the failure condition is written as

$$A_{\text{cert}} - A'_{\text{req}} < 0 \tag{C3}$$

The separable Monte Carlo simulation procedure is summarized in Fig. C1.

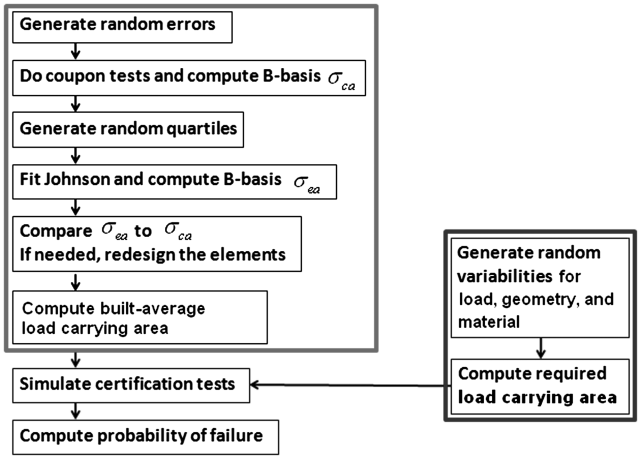


**Fig. C1 Flowchart for separable Monte Carlo simulations.**

## Acknowledgment

The author gratefully acknowledges the funding provided by The Scientific and Technological Research Council of Turkey (TÜBİTAK), under award MAG-109M537.

## References

[1] Lincoln, J. W., "Method for Computation of Structural Failure Probability for an Aircraft," Aeronautical Systems Div., TR-80-5035, Wright-Patterson AFB, OH, July 1980.

[2] Lincoln, J. W., "Risk Assessment of an Aging Aircraft," *Journal of Aircraft*, Vol. 22, No. 8, Aug. 1985, pp. 687–691. doi:10.2514/3.45187

[3] Shiao, M. C., Nagpal, V. K., and Chamis, C. C., "Probabilistic Structural Analysis of Aerospace Components Using NESSUS," AIAA Paper 88-2373, 1988.

[4] Wirsching, P. H., "Literature Review on Mechanical Reliability and Probabilistic Design," *Probabilistic Structural Analysis Methods for Select Space Propulsion System Components (PSAM)*, Vol. 3, NASA CR 189159, 1992.

[5] Lykins, C., Thomson, D., and Pomfret, C., "The Air Force's Application of Probablistics to Gas Turbine Engines," AIAA Paper 94-1440-CP, 1994.

[6] Ebberle, D. H., Newlin, L. E., Sutharshana, S., and Moore, N. R., "Alternative Computational Approaches for Probabilistic Fatigue

Analysis," AIAA Paper 95-1359, 1995.
[7] Ushakov, A., Kuznetsov, A. A., Stewart, A., and Mishulin, I. B., "Probabilistic Design of Damage Tolerant Composite Aircraft Structures," U.S. Dept. of Defense and Federal Aviation Administration, Rept. DOT/FAA/AR-01/55, 1996.
[8] Mavris, D. N., Macsotai, N. I., and Roth, B., "A Probabilistic Design Methodology for Commercial Aircraft Engine Cycle Selection," Society of Automotive Engineers, Paper 985510, 1998.
[9] Long, M. W., and Narciso, J. D., "Probabilistic Design Methodology for Composite Aircraft Structures," U.S. Dept. of Defense and Federal Aviation Administration, Rept. AR-99/2, June 1999.
[10] Rusk, D. T., Lin, K. Y., Swartz, D. D., and Ridgeway, G. K., "Bayesian Updating of Damage Size Probabilities for Aircraft Structural Life-Cycle Management," *Journal of Aircraft*, Vol. 39, No. 4, July 2002, pp. 689–696. doi:10.2514/2.2983
[11] Allen, M., and Maute, K., "Reliability-Based Design Optimization of Aeroelastic Structures," *Structural and Multidisciplinary Optimization*, Vol. 27, 2004, pp. 228–242. doi:10.1007/s00158-004-0384-1
[12] Huang, C. K., and Lin, K. Y., "A Method for Reliability Assessment of Aircraft Structures Subject to Accidental Damage," AIAA Paper 2005-1830, 2005.
[13] Nam, T., Soban, D. S., and Mavris, D. N., "A Non-Deterministic Aircraft Sizing Method Under Probabilistic Design Constraints," AIAA Paper 2006-2062, 2006.
[14] Lin, K. Y., and Styuart, A. V., "Probabilistic Approach to Damage Tolerance Design of Aircraft Composite Structures," *Journal of Aircraft*, Vol. 44, No. 4, July–Aug. 2007, pp. 1309–1317. doi:10.2514/1.26913
[15] Qu, X., Haftka, R. T., Venkataraman, S., and Johnson, T. F., "Deterministic and Reliability-Based Optimization of Composite Laminates for Cryogenic Environments," *AIAA Journal*, Vol. 41, No. 10, 2003, pp. 2029–2036. doi:10.2514/2.1893
[16] Acar, E., Haftka, R. T., Sankar, B. V. and Qui, X., "Increasing Allowable Flight Loads by Improved Structural Modeling," *AIAA Journal*, Vol. 44, No. 2, 2006, pp. 376–381. doi:10.2514/1.17804
[17] Acar, E., Haftka, R. T., and Johnson, T. F., "Tradeoff of Uncertainty Reduction Mechanisms for Reducing Structural Weight," *Journal of Mechanical Design*, Vol. 129, No. 3, 2007, pp. 266–274. doi:10.1115/1.2406097
[18] Li, M., Williams, N., and Azarm, S., "Interval Uncertainty Reduction and Sensitivity Analysis with Multi-Objective Design Optimization," *Journal of Mechanical Design*, Vol. 131, No. 3, 2009, Paper 031007. doi:10.1115/1.3066736
[19] Jiao, G., and Moan, T., "Methods of Reliability Model Updating Through Additional Events," *Structural Safety*, Vol. 9, No. 2, 1990, pp. 139–153. doi:10.1016/0167-4730(90)90005-A
[20] Jiao, G., and Eide, O. I., "Effects of Testing, Inspection and Repair on the Reliability of Offshore Structures," *Proceedings of the Seventh Specialty Conference*, Worcester, MA, Aug. 7–9 1996, pp. 154–157.
[21] Beck, J. L., and Katafygiotis, L. S., "Updating Models and Their Uncertainties: Bayesian Statistical Framework," *Journal of Engineering Mechanics*, Vol. 124, No. 4, 1998, pp. 455–461. doi:10.1061/(ASCE)0733-9399(1998)124:4(455)
[22] Papadimitriou, C., Beck, J. L., and Katafygiotis, L. S., "Updating Robust Reliability Using Structural Test Data," *Probabilistic Engineering Mechanics*, Vol. 16, No. 2, 2001, pp. 103–113. doi:10.1016/S0266-8920(00)00012-6
[23] Acar, E., Haftka, R. T., and Kim, N. H., "Effects of Structural Tests on Aircraft Safety," *AIAA Journal*, Vol. 48, No. 10, 2010, pp. 2235–2248. doi:10.2514/1.J050202
[24] Acar, E., Haftka, R. T., Kim, N. H., Turinay, M., and Park, C., "Reliability- Based Structural Design of Aircraft Together with Future Tests," 51th AIAA/ASME/ASCE/AHS/ASC Structures, Structural Dynamics, and Materials Conference, Orlando, FL, AIAA Paper 2010-2595, April 2010.
[25] Kaufmann, M., Zenkert, D., and Wennhage, P., "Integrated Cost/Weight Optimization of Aircraft Structures," *Structural and Multidisciplinary Optimization*, Vol. 41, No. 2, 2010, pp. 325–334. doi:10.1007/s00158-009-0413-1
[26] Curran, R., Rothwell, A., and Castagne, S., "Numerical Method for Cost-Weight Optimization of Stringer—Skin Panels," *Journal of Aircraft*, Vol. 43, No. 1, 2006, pp. 264–274. doi:10.2514/1.13225
[27] Kim, H. A., Kennedy, D., and Gürdal, Z., "Special Issue on Optimization of Aerospace Structures," *Structural and Multidisciplinary Optimization*, Vol. 36, No. 1, 2008, pp. 1–2. doi:10.1007/s00158-008-0256-1
[28] "Materials Research to Meet 21st Century Defense Needs," National Research Council, 2003.
[29] Jenkinson, L. R., Simpkin, P., and Rhodes, D., *Civil Jet Aircraft Design*, AIAA Education Series, AIAA, Reston, VA, 1999, pp. 134–135.
[30] Acar, E., "Guided Tail Modelling for Efficient and Accurate Reliability Estimation of Highly Safe Mechanical Systems," *Proceedings of the Institution of Mechanical Engineers Part C, Mechanical Engineering Science*, Vol. 225, No. 5, 2011, pp. 1237–1251. doi:10.1177/2041298310392833
[31] "Factor of Safety," *Code of Federal Regulations*, Pt. 25, Airworthiness Standards: Transport Category Airplanes, Sec. 25.303, Federal Aviation Administration, 1970.
[32] "Material Strength Properties and Material Design Value," *Code of Federal Regulations*, Part 25, Airworthiness Standards: Transport Category Airplanes, Sec. 25.613, Federal Aviation Administration, 2003.
[33] *Composite Materials Handbook*, Vol. 1, MIL-HDBK-17, U.S. Dept. of Defense, 2002, Chaps. 2, 8.
[34] "Proof of Structure," *Code of Federal Regulations*, Pt. 25, Airworthiness Standards: Transport Category Airplanes, Sec. 25.307, Federal Aviation Administration, 1990.
[35] Oberkampf, W. L., Deland, S. M., Rutherford, B. M., Diegert, K. V., and Alvin, K. F., "Estimation of Total Uncertainty in Modeling and Simulation," Sandia National Labs., Rept. SAND 2000-0824, Albuquerque, NM, 2000.
[36] Oberkampf, W. L., Deland, S. M., Rutherford, B. M., Diegert, K. V., and Alvin, K. F., "Error and Uncertainty in Modeling and Simulation," *Reliability Engineering and System Safety*, Vol. 75, 2002, pp. 333–357. doi:10.1016/S0951-8320(01)00120-X
[37] Acar, E., Kale, A., Haftka, R. T., and Stroud, W. J., "Structural Safety Measures for Airplanes," *Journal of Aircraft*, Vol. 43, No. 1, 2006, pp. 30–38. doi:10.2514/1.14381
[38] Acar, E., Kale, A., and Haftka, R. T., "Comparing Effectiveness of Measures that Improve Aircraft Structural Safety," *Journal of Aerospace Engineering*, Vol. 20, No. 3, 2007, pp. 186–199. doi:10.1061/(ASCE)0893-1321(2007)20:3(186)
[39] Antonsson, E. K., and Otto, K. N., "Imprecision in Engineering Design," *Journal of Mechanical Design*, Vol. 117, 1995, pp. 25–32. doi:10.1115/1.2836465
[40] Nikolaidis, E., Chen, S., Cudney, H., Haftka, R. T., and Rosca, R., "Comparison of Probability and Possibility for Design Against Catastrophic Failure Under Uncertainty," *Journal of Mechanical Design*, Vol. 126, 2004, pp. 386–394. doi:10.1115/1.1701878
[41] Owen, D. B., "Tables for Computing Bivariate Normal Probabilities," *Annals of Mathematical Statistics*, Vol. 27, 1956, pp. 1075–1090. doi:10.1214/aoms/1177728074
[42] Noh, Y., Choi, K. K., and Du, L., "Reliability-Based Design Optimization of Problems with Correlated Input Variables Using a Gaussian Copula," *Structural and Multidisciplinary Optimization*, Vol. 38, 2009, pp. 1–16. doi:10.1007/s00158-008-0277-9
[43] Smarslok, B. P., Haftka, R. T., Carraro, L., and Ginsbourger, D., "Improving Accuracy of Failure Probability Estimates with Separable Monte Carlo, " *International Journal of Reliability and Safety*, Vol. 4, 2010, pp. 393–414. doi:10.1504/IJRS.2010.035577